

Infrared Multiphoton Dissociation Spectroscopy of Cationized Threonine: Effects of Alkali-Metal Cation Size on Gas-Phase Conformation

M. T. Rodgers,^{*,†} P. B. Armentrout,^{*,‡} J. Oomens,[§] and J. D. Steill[§]

Department of Chemistry, Wayne State University, Detroit, Michigan 48202, Department of Chemistry, University of Utah, Salt Lake City, Utah 84112, and FOM Institute for Plasma Physics “Rijnhuizen”, Edisonbaan 14, 3439 MN Nieuwegein, The Netherlands

Received: November 27, 2007; In Final Form: December 19, 2007

The gas-phase structures of alkali-metal cation complexes of threonine (Thr) are examined using infrared multiple photon dissociation (IRMPD) spectroscopy utilizing light generated by a free electron laser in conjunction with quantum chemical calculations. Spectra of $\text{Li}^+(\text{Thr})$ and $\text{Na}^+(\text{Thr})$ are similar and relatively simple, whereas $\text{K}^+(\text{Thr})$, $\text{Rb}^+(\text{Thr})$, and $\text{Cs}^+(\text{Thr})$ include distinctive new IR bands. Measured IRMPD spectra are compared to spectra calculated at a B3LYP/6-311+G(d,p) level to identify the structures present in the experimental studies. For the smaller metal cations, the spectra match those predicted for charge-solvated structures in which the ligand exhibits tridentate coordination, $\text{M1}[\text{N},\text{CO},\text{OH}]$, binding to the amide and carbonyl groups of the amino acid backbone and to the hydroxyl group of the side chain. $\text{K}^+(\text{Thr})$, $\text{Rb}^+(\text{Thr})$, and $\text{Cs}^+(\text{Thr})$ exhibit evidence of the charge-solvated complex, $\text{M3}[\text{COOH}]$, in which the metal cation binds to the carboxylic acid group. Evidence for a small population of the zwitterionic analogue of this structure, $\text{ZW}[\text{CO}_2^-]$, is also present, particularly for the Cs^+ complex. Calculations indicate that the relative stability of the $\text{M3}[\text{COOH}]$ structure is very strongly dependent on the size of the metal cation, consistent with the range of conformations observed experimentally. The present results are similar to those obtained previously for the analogous $\text{M}^+(\text{Ser})$ complexes, although there are subtle distinctions that are discussed.

Introduction

It is known that sodium cations drive the transport of free serine (Ser) and threonine (Thr) and their peptide forms into an asaccharolytic, Gram-negative bacterium called porphyromonas gingivalis.¹ Therefore, a quantitative assessment of the pairwise interactions between amino acids and peptides with alkali-metal cations is potentially useful in understanding the thermodynamics of such processes. In a recent guided ion beam mass spectrometry study of the complexes of the alkali-metal cations, Li^+ , Na^+ , and K^+ , with Ser and Thr,² quantitative bond dissociation energies (BDEs) were found to be nearly identical for both ligands, consistent with their very similar structures (differing only by a methyl group). Likewise, a theoretical study of the possible conformations found BDEs in good agreement with experiment for the predicted ground-state conformers, charge-solvated structures involving tridentate binding to the amide and carbonyl groups of the amino acid backbone combined with interaction with the side-chain hydroxyl group, $\text{M1}[\text{N},\text{CO},\text{OH}]$ (see below for a definition of the nomenclature used). For these three $\text{M}^+(\text{Thr})$ complexes, the $\text{M1}[\text{N},\text{CO},\text{OH}]$ ground-state conformation is calculated to lie well below (>8 kJ/mol) any other conformations, such that quantitative bond energy measurements are sufficient to determine the identity of the complexes formed experimentally.² However, the energy gaps between the ground-state and excited conformations are calculated to narrow as the size of the metal cation increases such that alternate conformations may appear with the heavier

alkali-metal cations. Indeed, our recent infrared multiphoton dissociation (IRMPD) spectroscopy study of the related $\text{M}^+(\text{Ser})$ complexes, where $\text{M}^+ = \text{Li}^+$, Na^+ , K^+ , Rb^+ , and Cs^+ , found evidence for the bidentate $\text{M3}[\text{COOH}]$ conformation appearing in the potassium and rubidium complexes as well as the zwitterionic $\text{ZW}[\text{CO}_2^-]$ for the cesium complex.³ The additional methyl group in Thr compared to Ser could subtly shift the relative stabilities of these alternate isomers, a process that can be studied spectroscopically. In other similar work, IRMPD spectroscopy studies of $\text{M}^+(\text{Trp})$ ⁴ and $\text{M}^+(\text{Lys})$ ⁵ find a shift from charge-solvated tridentate to charge-solvated bidentate binding as the metal cation gets heavier, whereas IRMPD spectra of $\text{M}^+(\text{Arg})$ ⁶ show a transition between charge-solvated and zwitterionic structures occurring at $\text{M}^+ = \text{Na}^+$. In the present study, we measure the IRMPD action spectra for dissociation of the $\text{M}^+(\text{Thr})$ complexes, where $\text{M}^+ = \text{Li}^+$, Na^+ , K^+ , Rb^+ , and Cs^+ , and compare them to our findings for the analogous $\text{M}^+(\text{Ser})$ complexes. Identification of the conformations present is achieved by comparison to IR spectra derived from quantum chemical calculations of the low-lying structures of the $\text{M}^+(\text{Thr})$ complexes with optimized structures and vibrational frequencies determined at the B3LYP/6-311+G(d,p) level of theory.

Experimental and Computational Section

Mass Spectrometry and Photodissociation. A 4.7 T Fourier-transform ion cyclotron resonance (FTICR) mass spectrometer was used in these experiments and has been described in detail elsewhere.^{7–9} Tunable radiation for the photodissociation experiments is generated by the free electron laser for infrared experiments (FELIX).¹⁰ For the present experiments, spectra were recorded over the wavelength range from 19.4 (520 cm^{-1})

* To whom correspondence should be addressed.

† Wayne State University.

‡ University of Utah.

§ FOM Institute for Plasma Physics “Rijnhuizen”.

to 5.5 μm (1820 cm^{-1}). Pulse energies were around 50 mJ per macropulse of 5 μs duration, although they fell off to about 20 mJ toward the blue edge of the scan range. The fwhm bandwidth of the laser was typically 0.5% of the central wavelength. Threonine was obtained from Aldrich. Cationized amino acids were formed by electrospray ionization using a Micromass Z-Spray source and a solution of 3.0 mM amino acid and 0.5–1.0 mM alkali-metal chloride in 70%:30% MeOH/H₂O solutions. Solution flow rates ranged from 15 to 30 $\mu\text{L}/\text{min}$, and the electrospray needle was generally held at a voltage of ~ 3.2 kV. Ions were accumulated in a hexapole trap for about 4 s prior to being injected into the ICR cell via a radiofrequency (rf) octopole ion guide. Electrostatic switching of the dc bias of the octopole allows ions to be captured in the ICR cell without the use of a gas pulse, thus avoiding collisional heating of the ions.⁸ Ions were irradiated for 3 s, which corresponds to interaction with 15 macropulses.

Computational Details. In previous work,² Ye and Armentrout examined all likely conformers of threonine and its complexes with Li⁺, Na⁺, and K⁺ using a simulated annealing procedure that combines annealing cycles and quantum chemical calculations.¹¹ Briefly, the AMBER program and AMBER force field based on molecular mechanics¹² were used to search for possible stable structures in each system's conformational space. All possible structures identified in this way were further optimized using NWChem¹³ at the HF/3-21G level.^{14,15} Unique structures for each system within 50 kJ/mol of the lowest energy structure (~ 30 for each complex) were further optimized using Gaussian 03¹⁶ at the B3LYP/6-31G(d) level^{17,18} with "loose" optimization (maximum step size of 0.01 au and a rms force of 0.0017 au) to facilitate convergence. Because threonine has 2*S*,3*R* chirality, this property is constrained throughout the annealing simulations. The 10–15 lowest energy structures obtained from this procedure were then chosen for higher level geometry optimizations and frequency calculations using density functional theory (DFT) at the B3LYP/6-311+G(d,p) level.^{19,20} This level of theory has been shown to provide reasonably accurate structural descriptions of comparable metal–ligand systems.^{11,21} Single-point energy calculations were carried out for the 6–15 most stable structures at the B3LYP, B3P86, and MP2(full) levels using the 6-311+G(2d,2p) basis set.¹⁹ Zero-point vibrational energy (ZPE) corrections were determined using vibrational frequencies calculated at the B3LYP/6-311+G(d,p) level scaled by a factor of 0.9804.²²

For the Rb⁺ and Cs⁺ complexes studied here, all conformations considered previously for K⁺(Thr) were used as starting points for geometry and vibrational frequency calculations optimized at the B3LYP/HW*/6-311+G(d,p) level, where HW* indicates that Rb and Cs were described using the effective core potentials (ECPs) and valence basis sets of Hay and Wadt²³ with a single d polarization function (exponents of 0.24 and 0.19, respectively) included.²⁴ Relative energies were determined using single-point energies at the B3LYP, B3P86, and MP2(full) levels using the HW*/6-311+G(2d,2p) basis set. In our previous work on serine complexes,³ we performed similar HW* calculations for the K⁺(Ser) complexes (with an exponent of 0.48 for the d polarization function on K) in order to assess the accuracy of the Hay–Wadt ECP/valence basis sets. It was found that vibrational frequencies calculated using the all-electron vs HW* basis sets on K yield results that differ by an average of less than 0.03%. Hence, we did not perform HW* calculations on the K⁺(Thr) complex and conclude that use of the HW* basis sets for the Rb and Cs systems should yield equivalent results to the all-electron basis sets used for the smaller cations.

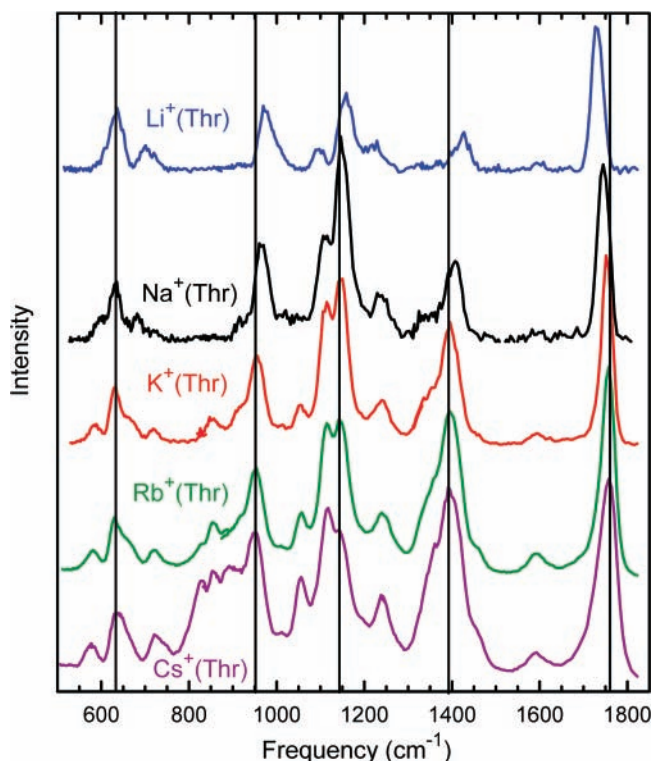


Figure 1. Infrared multiphoton dissociation action spectra of $M^+(\text{Thr})$ complexes, where $M^+ = \text{Li}^+, \text{Na}^+, \text{K}^+, \text{Rb}^+, \text{and Cs}^+$.

Vibrational frequencies and intensities were calculated using the harmonic oscillator approximation and analytical derivatives of the energy-minimized Hessian calculated at the B3LYP/6-311+G(d,p) or B3LYP/HW*/6-311+G(d,p) level of theory. Frequencies were scaled by 0.9804 to eliminate known systematic errors.²² For comparison to experiment, calculated vibrational frequencies are broadened using a 20 cm^{-1} fwhm Gaussian line shape. A detailed list of the theoretically predicted frequencies and IR intensities for the three main conformers of $M^+(\text{Thr})$ are provided as Tables S1–S3 in the Supporting Information. Table S4 provides this information for the remaining conformers of Li⁺(Thr).

Results and Discussion

IRMPD Action Spectroscopy. Photodissociation of $M^+(\text{Thr})$, where $M^+ = \text{K}^+, \text{Rb}^+, \text{and Cs}^+$, results in the loss of the intact ligand to form the atomic metal cation. This is consistent with collision-induced dissociation (CID) results for the potassium complexes² and with results for IRMPD on the analogous $M^+(\text{Ser})$ complexes.³ In these systems, IRMPD action spectra are taken from the relative intensity of the M^+ product ion as a function of laser wavelength and are shown in Figure 1. No corrections for laser power were applied but would primarily enhance the intensities observed at the highest laser frequencies.

For the Na⁺(Thr) complex, formation of the atomic metal cation is the dominant product observed, but product ions corresponding to losses of H₂O and CH₃CHO are also observed. The latter were not observed in the CID spectra,² suggesting that these channels are relatively low in energy but entropically disfavored, such that their production is enhanced by the slow heating afforded by IRMPD. The sum of the Na⁺, Na⁺(Thr–H₂O), and Na⁺(Thr–CH₃CHO) channels is shown as the IRMPD action spectrum in Figure 1. To a first approximation, the relative magnitudes are 60:30:10, respectively, but there are

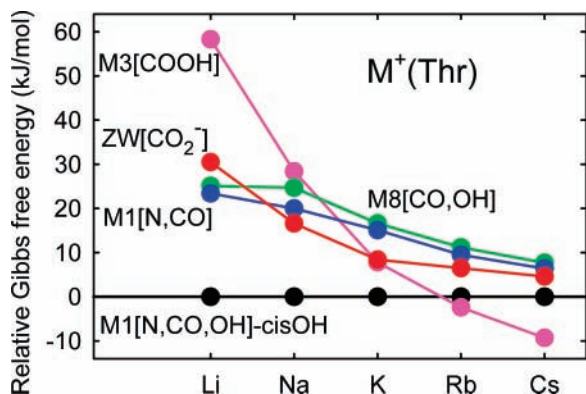


Figure 2. Gibbs free energies (kJ/mol) calculated at the B3LYP level of theory (Table 1) of five conformations of $M^+(\text{Thr})$ complexes as a function of the alkali-metal cation identity relative to the energy of the $M1[\text{N},\text{CO},\text{OH}]\text{-cisOH}$ conformer.

considerable variations in the relative intensities in different bands, as shown in Figure S1 in the Supporting Information. Chief among these is that formation of H_2O loss becomes relatively more important as the frequency decreases, such that the Na^+ and H_2O loss product channels have nearly equivalent intensities in the band at 640 cm^{-1} . In addition, there is a slight red shift in the band at 1750 cm^{-1} for loss of Na^+ compared to H_2O loss. In IRMPD spectroscopy, a slight red shift in absorption bands is often observed for higher energy dissociation channels as a result of an increased influence of vibrational anharmonicity.^{25,26}

In the case of $\text{Li}^+(\text{Thr})$, atomic Li^+ has a mass too low to be observed easily in the FTICR; however, the CID spectra exhibit two low-energy channels: loss of H_2O and loss of the isobaric CH_3CHO or CO_2 .² At somewhat higher energies, loss of two H_2O and $\text{CH}_3\text{CHO}/\text{CO}_2 + \text{H}_2\text{O}$ from the complex as well as formation of $\text{Li}^+(\text{H}_2\text{O})$ and $\text{Li}^+(\text{CH}_3\text{CHO})$ are also observed.² Upon photodissociation, loss of H_2O and CH_3CHO are observed with the high resolution of the FTICR finding no loss of carbon dioxide. The sum of these two channels is shown as the IRMPD action spectrum in Figure 1. Loss of CH_3CHO exhibits an intensity about twice that of H_2O loss throughout the observed spectrum, Figure S1, although there is a slight red shift in the 1730 cm^{-1} band for loss of H_2O compared to CH_3CHO loss. As noted above, this can be attributed to the influence of vibrational anharmonicity.

Comparison of the five spectra in Figure 1 shows that the features observed in the $\text{Li}^+(\text{Thr})$ spectrum are retained for all of the metal cation complexes but that new spectral features begin to appear for $\text{K}^+(\text{Thr})$ and become pronounced for $\text{Cs}^+(\text{Thr})$. The band at 1730 cm^{-1} shifts to the blue as the metal cation becomes heavier, as do the minor bands at 1100 and 1230 cm^{-1} . In contrast, those at 700 , 970 , and 1420 cm^{-1} shift to the red, and the bands at 640 , 1150 , and 1600 cm^{-1} shift very little. The band at 1160 cm^{-1} in the $\text{Li}^+(\text{Thr})$ spectrum shifts to the red for $\text{Na}^+(\text{Thr})$ but then remains relatively constant for complexes of the heavier metal cations.

Theoretical Results. A detailed discussion of the structures of threonine and its metal cation complexes with Li^+ , Na^+ , and K^+ can be found elsewhere.² As described above, complexes with Rb^+ and Cs^+ were calculated here at the B3LYP/HW*/6-311+G(d,p) level starting with the structures of all low-lying potassium complexes located previously, a total of seven conformations. The nomenclature used to identify these different structural isomers is taken from that established previously for $\text{Na}^+(\text{Gly})$.^{11,27,28} Briefly, neutral threonine is designated as Nx, where x indicates one of three main types of structural isomers

TABLE 1: Relative Energies at 0 K and Free Energies at 298 K (kJ/mol) of Low-Lying Conformers of $M^+(\text{Thr})^a$

complex	structure	B3LYP	B3P86	MP2(full)	
$\text{Li}^+(\text{Thr})$	$M1[\text{N},\text{CO},\text{OH}]\text{-cis-OH}$	0.0 (0.0)	0.0 (0.0)	0.0 (0.0)	
	$M1[\text{N},\text{CO}]$	25.5 (23.4)	24.6 (22.4)	30.9 (28.8)	
	$M1[\text{N},\text{CO},\text{OH}]\text{-trans-OH}$	26.1 (26.0)	25.6 (25.5)	26.8 (26.7)	
	$M8[\text{CO},\text{OH}]$	26.2 (25.1)	25.1 (24.0)	35.0 (33.9)	
	$M5[\text{N},\text{OH},\text{OH}]$	28.8 (28.5)	30.3 (30.0)	25.1 (24.8)	
	$ZW[\text{CO}_2^-]$	33.1 (30.5)	29.6 (27.0)	37.1 (34.4)	
	$\text{TS}(\text{M3-ZW})$	57.4 (55.6)	48.6 (46.7)	61.7 (59.9)	
	$M3[\text{COOH}]$	61.8 (58.3)	56.3 (52.8)	66.4 (62.9)	
	$\text{Na}^+(\text{Thr})$	$M1[\text{N},\text{CO},\text{OH}]\text{-cis-OH}$	0.0 (0.0)	0.0 (0.0)	0.0 (0.0)
		$ZW[\text{CO}_2^-]$	18.8 (16.6)	14.9 (12.8)	23.2 (21.1)
$M1[\text{N},\text{CO}]$		22.8 (20.0)	21.5 (18.7)	26.9 (24.2)	
$M1[\text{N},\text{CO},\text{OH}]\text{-trans-OH}$		26.2 (26.0)	25.7 (25.5)	26.8 (26.6)	
$M8[\text{CO},\text{OH}]$		26.5 (24.7)	24.0 (22.2)	32.3 (30.6)	
$M5[\text{N},\text{OH},\text{OH}]$		29.0 (28.9)	28.7 (28.6)	24.4 (24.3)	
$\text{TS}(\text{M3-ZW})$		30.9 (29.5)	21.4 (20.0)	34.4 (33.0)	
$M3[\text{COOH}]$		31.7 (28.4)	26.5 (23.1)	34.8 (32.4)	
$\text{K}^+(\text{Thr})$		$M1[\text{N},\text{CO},\text{OH}]\text{-cis-OH}$	0.0 (0.0)	0.0 (0.0)	0.0 (0.0)
		$ZW[\text{CO}_2^-]$	10.1 (8.4)	6.3 (4.7)	17.8 (16.1)
	$M3[\text{COOH}]$	11.1 (7.8)	7.8 (4.5)	17.4 (14.1)	
	$\text{TS}(\text{M3-ZW})$	14.6 (13.2)	6.3 (4.8)	21.3 (19.8)	
	$M1[\text{N},\text{CO}]$	17.6 (15.1)	16.2 (13.6)	22.1 (19.6)	
	$M8[\text{CO},\text{OH}]$	18.9 (16.6)	16.6 (14.4)	25.7 (23.4)	
	$M1[\text{N},\text{CO},\text{OH}]\text{-trans-OH}$	24.8 (24.3)	24.7 (24.4)	25.8 (25.4)	
	$M5[\text{N},\text{OH},\text{OH}]$	25.5 (25.0)	26.9 (26.4)	23.2 (22.8)	
	$\text{Rb}^+(\text{Thr})$	$M1[\text{N},\text{CO},\text{OH}]\text{-cis-OH}$	0.0 (2.4)	2.3 (5.5)	0.0 (0.0)
		$M3[\text{COOH}]$	0.9 (0.0)	0.0 (0.0)	10.2 (6.9)
$ZW[\text{CO}_2^-]$		8.1 (8.9)	6.5 (8.2)	19.3 (17.8)	
$\text{TS}(\text{M3-ZW})$		8.2 (8.9)	2.1 (3.7)	18.0 (16.3)	
$M1[\text{N},\text{CO}]$		12.6 (11.9)	14.6 (14.8)	20.6 (17.6)	
$M8[\text{CO},\text{OH}]$		14.2 (13.6)	15.0 (15.3)	23.2 (20.3)	
$M5[\text{N},\text{OH},\text{OH}]$		24.3 (26.0)	27.4 (30.1)	21.4 (20.8)	
$M1[\text{N},\text{CO},\text{OH}]\text{-trans-OH}$		24.6 (26.7)	26.6 (29.5)	25.3 (25.0)	
$\text{Cs}^+(\text{Thr})$		$M3[\text{COOH}]$	0.0 (0.0)	0.0 (0.0)	4.3 (0.7)
		$M1[\text{N},\text{CO},\text{OH}]\text{-cis-OH}$	5.7 (9.3)	8.4 (11.9)	0.0 (0.0)
	$\text{TS}(\text{M3-ZW})$	10.2 (11.8)	4.8 (6.5)	15.2 (12.5)	
	$ZW[\text{CO}_2^-]$	12.1 (13.9)	10.8 (12.7)	18.1 (16.3)	
	$M1[\text{N},\text{CO}]$	15.2 (15.7)	17.9 (18.4)	17.3 (14.2)	
	$M8[\text{CO},\text{OH}]$	16.9 (17.0)	18.3 (18.5)	20.3 (16.8)	
	$M5[\text{N},\text{OH},\text{OH}]$	29.0 (31.4)	32.4 (34.8)	21.4 (20.2)	
	$M1[\text{N},\text{CO},\text{OH}]\text{-trans-OH}$	29.8 (32.7)	32.2 (35.1)	24.7 (24.0)	

^a Free energies are in parentheses. All values calculated at the level of theory indicated using the 6-311+G(2d,2p) basis set with structures and zero-point energies calculated at the B3LYP/6-311+G(d,p) level of theory. Values for Rb and Cs use the HW* basis set on the metal. The ground-state conformer is indicated in bold face.

with different modes of intramolecular hydrogen bonding. This is followed by a notation that indicates the relative position (either trans = t or gauche = g) of the $-\text{OH}$ group to the carbonyl carbon and its position relative to the amino nitrogen. Conformations of $M^+(\text{Thr})$ are identified as M_y (where y refers to a specific structure as first designated by Jensen for glycine complexes²⁹) augmented by a notation in brackets that describes the metal binding sites for each isomer. The zwitterionic conformer is designated as $ZW[\text{CO}_2^-]$.

Single-point energies including zero-point energy (ZPE) corrections calculated at three different levels of theory, relative to the lowest energy isomer, are given in Table 1 for $M^+(\text{Thr})$. Because the relative Gibbs free energies at 298 K may be more relevant in the determination of the experimental distribution, these values are also listed in Table 1. Figure 2 shows the overall trends in the relative $\Delta_{298}G$ values (B3LYP results), which are very similar to those of the relative Δ_0H values. The main differences arise because the tridentate binding conformers, $M1[\text{N},\text{CO},\text{OH}]$ and $M5[\text{N},\text{OH},\text{OH}]$, have smaller entropic contributions compared to the bidentate binding conformers, such that they become 2–4 kJ/mol less stable. The other levels of theory show similar trends as those in Figure 2, although

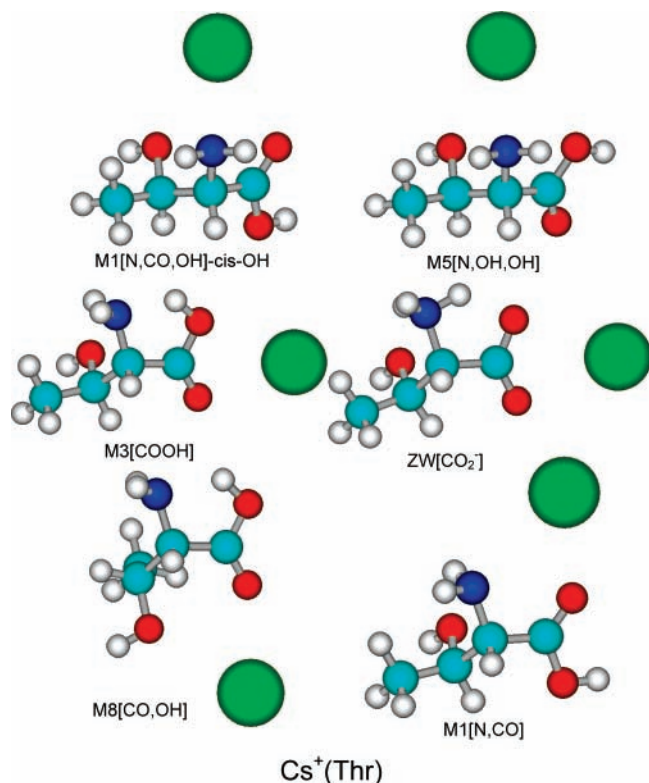


Figure 3. Structures of the $\text{Cs}^+(\text{Thr})$ complexes calculated at the B3LYP/HW*/6-311+G(d,p) level of theory.

the relative stability of the $\text{M1}[\text{N,CO,OH}]\text{-cis-OH}$ conformer is enhanced at the MP2(full) level.

The N2-gg structure is the ground-state conformer of threonine at all three levels of theory.² Five other low-lying conformations (N1-tg, N1-gg, N2-gt, N2-tg, and N3-tg) have also been described and are found to lie within 9 kJ/mol at all levels of theory.² The N2 type of structure is characterized by a $\text{COH}\cdots\text{N}$ hydrogen bond (1.91 Å) with an additional $\text{C}_\beta\text{O}\cdots\text{HN}$ hydrogen bond (2.48 Å) and a third long-distance (2.79 Å) $\text{C}_\beta\text{OH}\cdots\text{O}=\text{C}$ hydrogen bond.

Figure 3 illustrates the low-lying structures found for all $\text{M}^+(\text{Thr})$ complexes as exemplified by $\text{Cs}^+(\text{Thr})$. Table 2 lists several important geometric parameters for the $\text{M}^+(\text{Thr})$ complexes. The ground-state structure for most of the alkali-metal cations is the tridentate charge-solvated $\text{M1}[\text{N,CO,OH}]\text{-cis-OH}$ conformer, where *cis-OH* indicates that the carboxylic hydrogen is *cis* relative to the carbonyl oxygen. As the metal cation varies from Li^+ to Cs^+ , the $\text{M}^+\text{-OC}$, $\text{M}^+\text{-N}$, and $\text{M}^+\text{-OH}$ distances are calculated to increase from 1.97 to 3.16 Å, 2.08 to 3.36 Å, and 1.96 to 3.23 Å, respectively. These changes directly reflect the increase in the ionic radius of the metal cation (0.70 Å for Li^+ , 0.98 Å for Na^+ , 1.33 Å for K^+ , 1.49 Å for Rb^+ , and 1.69 Å for Cs^+)³⁰ coupled with the resultant decreasing charge density, which weakens the electrostatic interaction with threonine. Likewise, the $\angle\text{M}^+\text{OC}$ bond angle increases with the size of the cation, consistent with elongations of the $\text{M}^+\text{-OC}$ and $\text{M}^+\text{-N}$ distances. The $\angle\text{M}^+\text{OCC}_\alpha$ and $\angle\text{NC}_\alpha\text{CO}$ dihedral angles increase and decrease, respectively, for the same reasons. This can be understood by realizing that the three ligating groups move closer to the metal cation the higher its charge density, such that the $\angle\text{M}^+\text{OCC}_\alpha$ dihedral angle for $\text{M}^+(\text{Thr})$ becomes more planar as the metal cation gets smaller, Table 2.

For $\text{Cs}^+(\text{Thr})$ and $\text{Rb}^+(\text{Thr})$, the DFT calculations indicate that the $\text{M3}[\text{COOH}]$ conformer is the ground state (or nearly

the ground state), Table 1, whereas the MP2(full) calculations continue to predict the $\text{M1}[\text{N,CO,OH}]\text{-cis-OH}$ conformer as the ground state. The $\text{M3}[\text{COOH}]$ and $\text{ZW}[\text{CO}_2^-]$ conformations are closely related, the main difference being the location of the proton bridging the COH and amine groups, Figure 3. Transition states (TSs) between $\text{M3}[\text{COOH}]$ and $\text{ZW}[\text{CO}_2^-]$ were located using the synchronous transit-guided quasi-Newton (STQN) method of Schlegel and co-workers³¹ or relaxed potential-energy surface scans at the B3LYP/HW*/6-311+G(d,p) level. Single-point energies for the TSs were calculated at the three levels listed above using the 6-311+G(2d,2p) or HW*/6-311+G(2d,2p) basis sets, and the relative energies after ZPE corrections are listed in Table 1. For $\text{Li}^+(\text{Thr})$, ZW is lower than the M3 conformer by 26–29 kJ/mol, with the TS between the two lying lower than the M3 conformer once ZPE corrections are made. Thus, the $\text{M3}[\text{COOH}]$ complex of $\text{Li}^+(\text{Thr})$ collapses to the lower energy $\text{ZW}[\text{CO}_2^-]$ with no barrier to the proton transfer. The $\text{Na}^+(\text{Thr})$ complex behaves similarly, with ZW lying 11–13 kJ/mol lower than M3 and the TS lying below M3 (although the free energies of the TS lie slightly above M3 at the B3LYP and MP2(full) levels of theory, Table 1). For $\text{K}^+(\text{Thr})$, the ZW and M3 conformers are nearly isoenergetic, lying within 2 kJ/mol of one another at all three levels of theory. Here the TS lies between 0 and 5 kJ/mol above ZW such that a barrier is observed for the proton transfer, except at the B3P86 level of theory. For the heavier metals, M3 is now clearly favored at all levels of theory such that ZW lies above M3 by 6–9 and 11–14 kJ/mol for $\text{Rb}^+(\text{Thr})$ and $\text{Cs}^+(\text{Thr})$, respectively. Energies for these TSs with ZPE corrections included were calculated to be 0–5 and 2–6 kJ/mol lower in energy than the $\text{ZW}[\text{CO}_2^-]$ conformer for $\text{M}^+ = \text{Rb}^+$ and Cs^+ , respectively. Thus, once ZPEs are included, the $\text{ZW}[\text{CO}_2^-]$ complexes of $\text{Rb}^+(\text{Thr})$ and $\text{Cs}^+(\text{Thr})$ collapse to the lower energy $\text{M3}[\text{COOH}]$ conformer.

Four alternative conformations of the $\text{M}^+(\text{Thr})$ complexes were also identified. They all remain at least 12 kJ/mol higher in energy than the ground-state conformer, Table 1, and their relative energies vary much less with metal cation identity than $\text{M3}[\text{COOH}]$ or $\text{ZW}[\text{CO}_2^-]$, Figure 2. These alternative conformations include $\text{M1}[\text{N,CO,OH}]\text{-trans-OH}$, which is almost identical to $\text{M1}[\text{N,CO,OH}]\text{-cis-OH}$ except that the carboxylic hydrogen is *trans* to the carbonyl oxygen. This breaks the intramolecular hydrogen bond between them, which costs nearly the same amount of energy for all five metal cations, 24–27 kJ/mol. By removing the $\text{M}^+\text{-OH}$ side-chain interaction but retaining the metal cation interaction with the backbone groups, the $\text{M1}[\text{N,CO}]$ bidentate conformer is obtained, Figure 3. This conformer lies 24–31, 21–27, 16–22, 12–21, and 15–18 kJ/mol above $\text{M1}[\text{N,CO,OH}]\text{-cis-OH}$ for Li^+ – Cs^+ , respectively, Table 1. These changes in the relative energies with metal cation identity reflect the stronger binding to the smaller cations. Because of the reduced steric constraints, these bidentate structures have $\text{M}^+\text{-OC}$ bond distances that are shorter by ~ 0.10 Å than the $\text{M1}[\text{N,CO,OH}]\text{-cis-OH}$ conformer for all five metal cations. In contrast, the relative $\text{M}^+\text{-N}$ distances vary as a function of the metal cation, decreasing by 0.05 and 0.02 for Li^+ and Na^+ , respectively, but increasing by 0.02, 0.05, and 0.08 Å for K^+ , Rb^+ , and Cs^+ , respectively. These changes occur despite the relaxed steric constraints and can be explained by a weakening of the metal cation interaction with the amino group compared to the other functional groups as the metal cation size increases. This trend has previously been noted in our analysis of the interactions of $\text{Na}^+(\text{Gly})$ and $\text{K}^+(\text{Gly})$ complexes.^{11,21}

TABLE 2: Geometric Parameters of B3LYP/6-311+G(d,p) Geometry-Optimized Structures of M⁺(Thr)^a

conformer	$r(\text{M}^+-\text{O})$ (Å) ^b					$r(\text{M}^+-\text{N})$ (Å)					$r(\text{M}^+-\text{O})$ (Å)				
	Li	Na	K	Rb	Cs	Li	Na	K	Rb	Cs	Li	Na	K	Rb	Cs
M1[N,CO,OH]- <i>cis</i> -OH	1.968	2.318	2.666	2.919	3.155	2.083	2.443	2.851	3.129	3.364	1.961	2.332	2.726	2.997	3.229
M3[COOH]	1.911	2.286	2.635	2.902	3.119						2.091	2.420	2.838	3.099	3.360
ZW[CO ₂ ⁻]	1.929	2.286	2.624	2.891	3.101						1.957	2.314	2.676	2.935	3.170
M1[N,CO,OH]- <i>trans</i> -OH	1.940	2.288	2.624	2.870	3.087	2.101	2.470	2.896	3.190	3.452	1.965	2.334	2.737	3.012	3.258
M1[N,CO]	1.853	2.218	2.562	2.819	3.030	2.030	2.426	2.872	3.176	3.442					
M5[N,OH,OH]	2.014	2.383	2.809	3.090	3.384	2.048	2.409	2.806	3.082	3.321	1.929	2.294	2.672	2.936	3.161
M8[CO,OH]	1.810	2.169	2.508	2.756	2.969						1.895	2.300	2.738	3.039	3.309

conformer	$\angle\text{M}^+\text{OC}$ (deg)					$\angle\text{M}^+\text{OCC}_\alpha$ (deg)					$\angle\text{NC}_\alpha\text{CO}$ (deg)				
	Li	Na	K	Rb	Cs	Li	Na	K	Rb	Cs	Li	Na	K	Rb	Cs
M1[N,CO,OH]- <i>cis</i> -OH	103.3	107.6	112.3	114.0	114.7	11.9	19.4	28.4	34.5	39.4	32.6	27.4	21.0	16.9	13.4
M3[COOH]	93.2	96.8	102.1	104.0	106.6	178.1	177.9	176.3	176.9	176.3	175.9	176.0	175.6	175.5	175.2
ZW[CO ₂ ⁻]	84.0	88.6	92.7	94.5	96.6	178.3	178.5	178.4	178.1	178.5	169.6	170.3	170.8	171.0	171.2
M1[N,CO,OH]- <i>trans</i> -OH	105.7	110.6	116.0	118.0	119.5	10.6	18.2	27.2	34.1	40.1	34.3	29.2	23.4	19.1	15.7
M1[N,CO]	113.6	119.9	127.4	130.7	133.8	0.2	2.5	6.8	10.8	13.8	6.6	5.3	4.4	3.6	2.1
M5[N,OH,OH]	105.7 ^c	108.8 ^c	110.8 ^c	111.1 ^c	110.1 ^c	16.3 ^d	25.8 ^d	35.9 ^d	42.0 ^d	47.4 ^d	151.8	157.6	164.5	168.4	172.5
M8[CO,OH]	128.1	136.2	144.3	148.3	151.0	5.4	3.9	0.7	1.3	6.0	172.8	173.0	172.9	172.4	173.0

^a Values calculated at the B3LYP/6-311+G(d,p) or B3LYP/HW*/6-311+G(d,p) (italics) levels of theory. ^b The carbonyl oxygen in all cases except M5[N,OH,OH], where it is the carboxylic oxygen. ^c $\angle\text{M}^+\text{O}(\text{H})\text{C}_\alpha$ (deg). ^d $\angle\text{M}^+\text{O}(\text{H})\text{CC}_\alpha$ (deg).

In another tridentate isomer, M5[N,OH,OH], M⁺ binds to the hydroxyl oxygen of the carboxylic group instead of the carbonyl oxygen, Figure 3. This less favorable interaction^{11,21,32} leads to excitation energies of 21–30 kJ/mol above the M1-[N,CO,OH]-*cis*-OH conformer, with only a slight dependence on metal cation identity. The M⁺-N and side-chain M⁺-OH bond lengths are slightly shorter than in the M1 conformer, by 0.03–0.05 and 0.04–0.07 Å, respectively, whereas the backbone M⁺-OH bond length of M5 is appreciably longer than the M⁺-OC bond length of M1, by 0.05 for Li⁺ up to 0.23 for Cs⁺, Table 2. In the M8[CO,OH] structure, Figure 3, the metal cation binds to the carbonyl and side-chain hydroxyl oxygen atoms. The energy of this conformer remains at least 11 kJ/mol higher than the M1[N,CO,OH]-*cis*-OH conformer, but its relative stability drops by about 15 kJ/mol in going from Li⁺(Thr) to Cs⁺(Thr).

As shown in Figure 2, the relative energies for most conformations do not change appreciably as the metal cation changes. The obvious exception is the M3[COOH] conformer, which drops drastically as the metal cation gets larger and more diffuse. Previous work has calculated that the M3[COOH] conformer is the ground-state structure of K⁺(Gly),²¹ whereas M1[N,CO] is the ground state for Li⁺(Gly) and Na⁺(Gly).^{11,32,33} This difference in the preferred binding geometry has been attributed to relatively stronger interactions with the amino group as the metal cation gets smaller (higher charge density).²¹ For Thr, the metal cation interacts with the side-chain hydroxyl group as well as with the amino and carbonyl groups of the backbone. Therefore, the tridentate M1[N,CO,OH] conformation of M⁺(Thr) is stabilized relative to the bidentate M3[COOH] conformation. This shifts the change in ground-state conformation between M1 and M3 from a transition point between Na⁺(Gly) and K⁺(Gly) to the heavier metals for M⁺(Thr), Figure 2. A similar conclusion was reached in our previous exploration of the related M⁺(Ser) complexes.³

Comparison of Experimental and Theoretical IR Spectra: Li⁺(Thr). Figure 4 compares the experimental IRMPD action spectrum of Li⁺(Thr) with calculated IR spectra for the seven low-energy conformers listed in Table 1. Because the theoretical IR intensities are based on single photon absorption, predictions of IR intensities may not be in direct accord with the IRMPD action spectrum because the latter is a multiphoton process. Nevertheless, the bands predicted for the ground-state

M1[N,CO,OH]-*cis*-OH conformer correspond very well with the observed spectrum, both in terms of band position and generally relative band intensity.

The major band observed at 1730 cm⁻¹ corresponds to the carbonyl stretch, which explains its large predicted intensity. A band at essentially the same frequency was also found for the Li⁺(Ser) complex,³ indicating that the metal cation binds similarly to the carbonyl in both systems. This band is red shifted compared to free Thr, calculated as 1788 cm⁻¹ for N2-gg. A similar band is found for all of the Li⁺(Thr) conformations except M5[N,OH,OH] and ZW[CO₂⁻]. In the M5 conformer, the metal cation no longer binds to the carbonyl group, in contrast to all other conformations, resulting in a CO stretch that is blue shifted from that of bare Thr. For the zwitterion, the shift to a carboxylate leads to a CO stretch that is red shifted even further than for the M1 ground state.

The experimentally observed bands at 640, 970, and 1160 cm⁻¹ with shoulders at 700, 1090, and 1230 cm⁻¹ are probably the most diagnostic bands for the M1[N,CO,OH]-*cis*-OH structure. The positions and relative intensities of these bands are nicely predicted by the IR spectrum for this conformer, whereas no other conformation is predicted to have this same set of frequencies. Indeed, the spectrum would be even better predicted if bands at 733 and 1009 cm⁻¹ had intensities about one-half of those calculated. The sequence of bands observed between 1300 and 1500 cm⁻¹ are also consistent with the M1-[N,CO,OH]-*cis*-OH structure but are less characteristic as other conformers (notably M3[COOH], ZW[CO₂⁻], and M8[CO,OH]) have similar bands.

The biggest difference between the observed and predicted IR spectra involves the small peak observed at ~1600 cm⁻¹ in the IRMPD spectrum. In contrast, the M1[N,CO,OH]-*cis*-OH spectrum has a predicted band at 1630 cm⁻¹, as do many of the other conformers, Figure 4. The closest match is for M3-[COOH], which has a predicted frequency of 1608 cm⁻¹. In all conformations, this band corresponds primarily to a NH₂ bend and is largely unperturbed from the 1620 cm⁻¹ band predicted for neutral Thr (N2-gg). It seems likely that the harmonic approximation of the calculated potential gives somewhat inaccurate vibrational frequencies for this particular mode, as observed for NH₂ bending modes in other systems.^{25,34} A comparable observation was made in our study of the M⁺(Ser) complexes.³

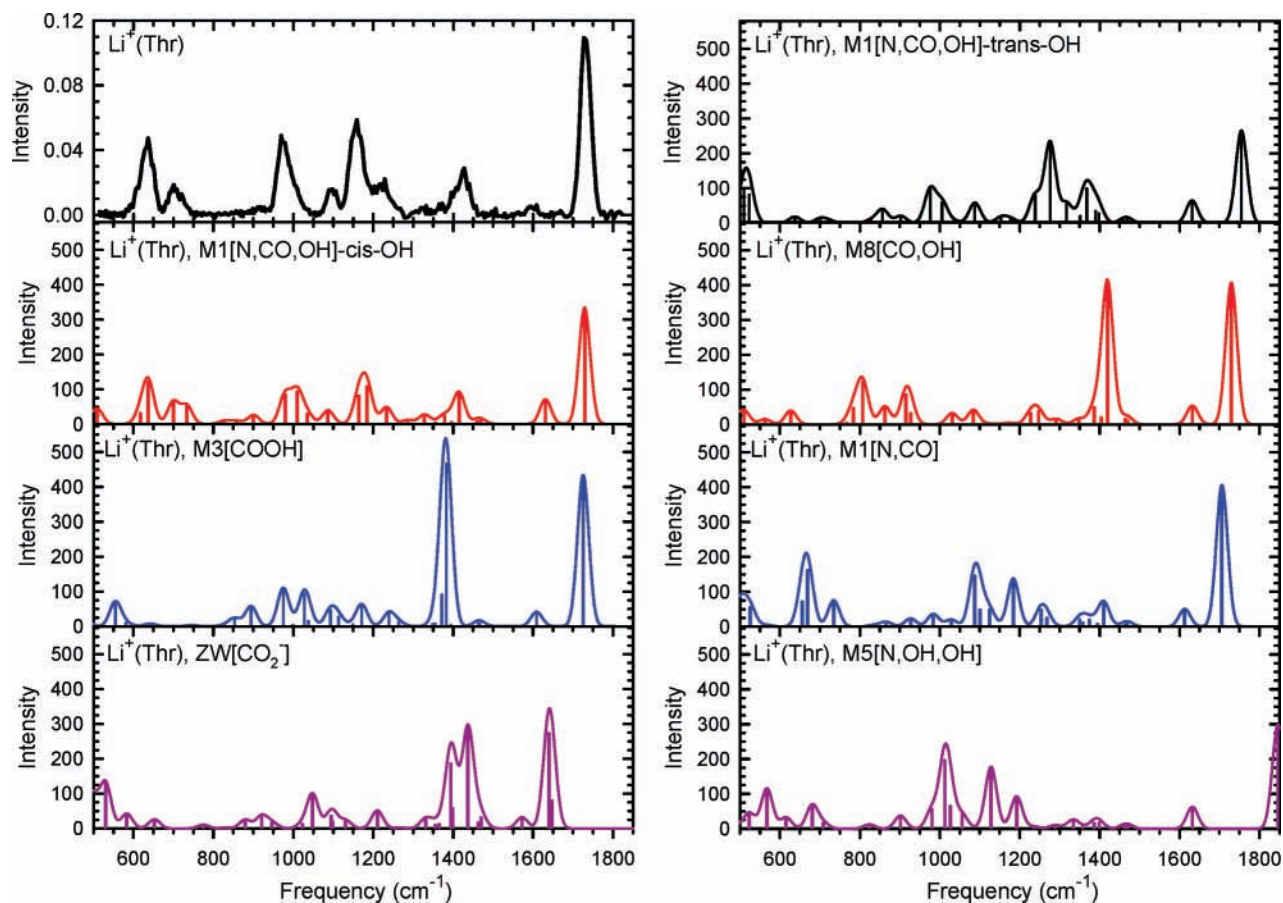


Figure 4. Comparison of the experimental IRMPD action spectrum for $\text{Li}^+(\text{Thr})$ with IR spectra for seven conformations predicted at the B3LYP/6-311+G(d,p) level of theory.

Comparison of Experimental and Theoretical IR Spectra: $\text{Na}^+(\text{Thr})$. Figure 1 shows that the IRMPD action spectra for $\text{Li}^+(\text{Thr})$ and $\text{Na}^+(\text{Thr})$ are very similar, exhibiting all of the same major spectral features. Comparison of experimental and theoretical spectra for $\text{Na}^+(\text{Thr})$ can be found in the Supporting Information, Figure S2. There are some subtle differences in the spectra for the two complexes, including a blue shift in the band at $\sim 1730\text{ cm}^{-1}$ (to $\sim 1745\text{ cm}^{-1}$) and an increase in intensity in shoulders to the low-frequency side of the bands at 640, 970, and 1420 cm^{-1} (although some intensity in this region seems to exist in the $\text{Li}^+(\text{Thr})$ spectrum). All of the observed features match the calculated spectrum for the M1-[N,CO,OH]-*cis*-OH conformer of $\text{Na}^+(\text{Thr})$, with agreement comparable to that obtained for $\text{Li}^+(\text{Thr})$. The calculated spectra correctly predict a blue shift in the 1730 cm^{-1} band of 14 cm^{-1} . The observed intensities of the bands at 1090 and 1150 cm^{-1} are about four and two times, respectively, more intense than predicted relative to the CO stretch, whereas most of the other bands have relative intensities comparable to the calculated spectrum. The increased intensity of the low-frequency shoulders compared to the $\text{Li}^+(\text{Thr})$ spectrum is probably a consequence of the improved sensitivity associated with the more weakly bound $\text{Na}^+(\text{Thr})$ vs $\text{Li}^+(\text{Thr})$ complex.² The Na^+-Thr BDE has been measured as $204 \pm 10\text{ kJ/mol}$ as compared with a Li^+-Thr BDE of $285 \pm 13\text{ kJ/mol}$ ² or the loss of H_2O and CH_3CHO from $\text{Li}^+(\text{Thr})$ of 191 ± 14 and $179 \pm 14\text{ kJ/mol}$, respectively.³⁵

Comparison of Experimental and Theoretical IR Spectra: $\text{K}^+(\text{Thr})$ and $\text{Rb}^+(\text{Thr})$. The IRMPD action spectrum of $\text{K}^+(\text{Thr})$ is similar to that of $\text{Na}^+(\text{Thr})$, Figure 1, with new peaks appearing at 720, 850, and 1050 cm^{-1} . In addition, there is a

notable increase in the relative intensity of the peaks at 1120 and 1400 cm^{-1} . The appearance of the new bands could be evidence for new conformers or could be the result of better sensitivity associated with more facile dissociation of this more weakly bound system. The K^+-Thr bond energy of $149 \pm 9\text{ kJ/mol}$ is substantially weaker than that for Na^+-Thr , $204 \pm 10\text{ kJ/mol}$.² The spectrum for $\text{Rb}^+(\text{Thr})$ is similar to that for $\text{K}^+(\text{Thr})$, Figure 1, with the same new bands compared to the $\text{Na}^+(\text{Thr})$ spectrum. The calculated bond energy for $\text{Rb}^+(\text{Thr})$, $103\text{--}122\text{ kJ/mol}$, is weaker than that for $\text{K}^+(\text{Thr})$, which again could lead to enhanced sensitivity.

Clearly, the ground-state M1[N,CO,OH]-*cis*-OH conformation continues to explain the bulk of the observed spectrum, as can be seen from the comparison in Figure 5. (Comparison of experimental and theoretical spectra for $\text{Rb}^+(\text{Thr})$ can be found in the Supporting Information, Figure S4.) Indeed, the M1 conformer does have bands at ~ 720 , 850, and 1050 cm^{-1} , although these are predicted to be relatively weak in the M1 spectra. Their appearance would then be attributed to the increased sensitivity associated with these more weakly bound complexes. However, the ZW[CO_2^-] and M3[COOH] conformers should also be considered as they are predicted to be low in energy, 6–19 kJ/mol higher for ZW for both metal cations, 8–17 kJ/mol higher for M3 of $\text{K}^+(\text{Thr})$, and 2 kJ/mol lower to 10 kJ/mol higher for M3 of $\text{Rb}^+(\text{Thr})$, Table 1. Figure 5 includes theoretical predictions for these two conformations as well.

One dominant feature in the predicted spectrum for M3[COOH] overlaps directly with the CO stretch feature in the M1[N,CO,OH]-*cis*-OH spectrum at 1750 cm^{-1} . The other obvious band in the M3[COOH] spectrum is the large feature at 1400 cm^{-1} , which could explain the increased intensity

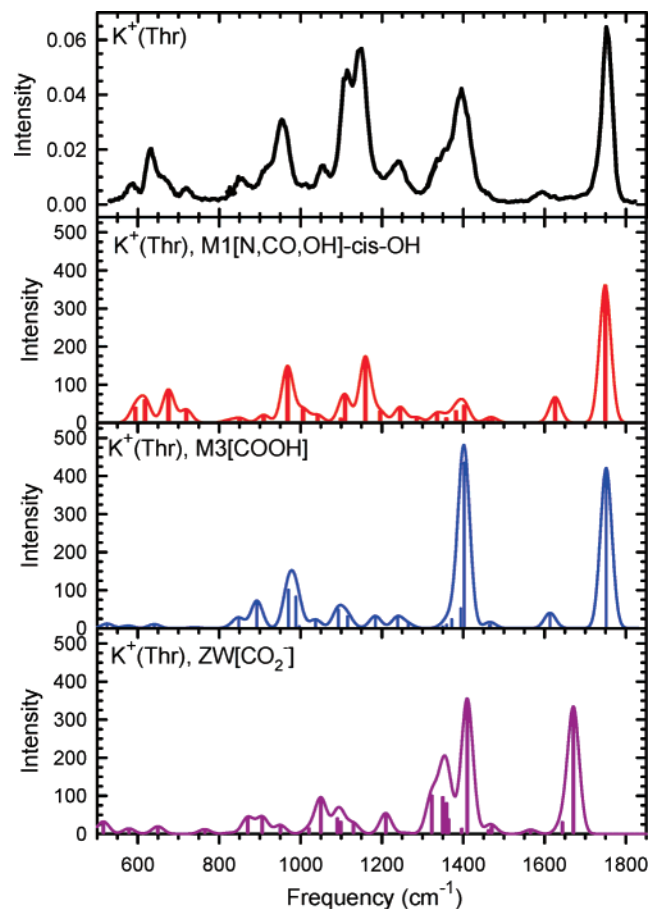


Figure 5. Comparison of the experimental IRMPD action spectrum for $K^+(\text{Thr})$ with IR spectra for three low-lying conformations predicted at the B3LYP/6-311+G(d,p) level of theory.

observed in the band at 1400 cm^{-1} . Other bands in the M3[COOH] spectrum in the range of $800\text{--}1200\text{ cm}^{-1}$ overlap the comparable bands in the M1[N,CO,OH]-*cis*-OH spectrum, although it is possible that the band at 850 cm^{-1} helps explain the appearance of this new band and the band at $\sim 1090\text{ cm}^{-1}$ helps explain the enhanced intensity of this band. The new bands at 720 and 1050 cm^{-1} do not appear to correspond particularly well with the predicted M3 spectra. However, the ZW conformer has appreciable intensity at a frequency of 1050 cm^{-1} , which could explain the appearance of this band. Further, the ZW bands between 1300 and 1400 cm^{-1} overlap the experimental peak observed in this region as well. The presence of the zwitterionic structure should be signaled most easily by the CO stretching band located at 1671 and 1684 cm^{-1} for $K^+(\text{Thr})$ and $Rb^+(\text{Thr})$, respectively. Certainly, no obvious peak appears in either spectrum, although there is an increase in intensity in this region of both spectra, perhaps suggesting the presence of a small amount of this conformer.

Comparison of Experimental and Theoretical IR Spectra: $Cs^+(\text{Thr})$. The IRMPD action spectrum of $Cs^+(\text{Thr})$ is clearly the most complicated of all five metal cation systems, Figure 1. Figure 6 compares the experimental spectrum with those calculated for the three most stable conformers. Compared to the $Rb^+(\text{Thr})$ spectrum, the biggest changes lie in the region between 800 and 1000 cm^{-1} . No new peaks are necessarily found, but the peaks at 830 and 890 cm^{-1} are more pronounced. The retention of the major features observed in the spectra for the smaller metal cations indicates that the M1[N,CO,OH]-*cis*-OH continues to be present. The presence of the M3[COOH] conformer is also likely, and a further increase in the intensity

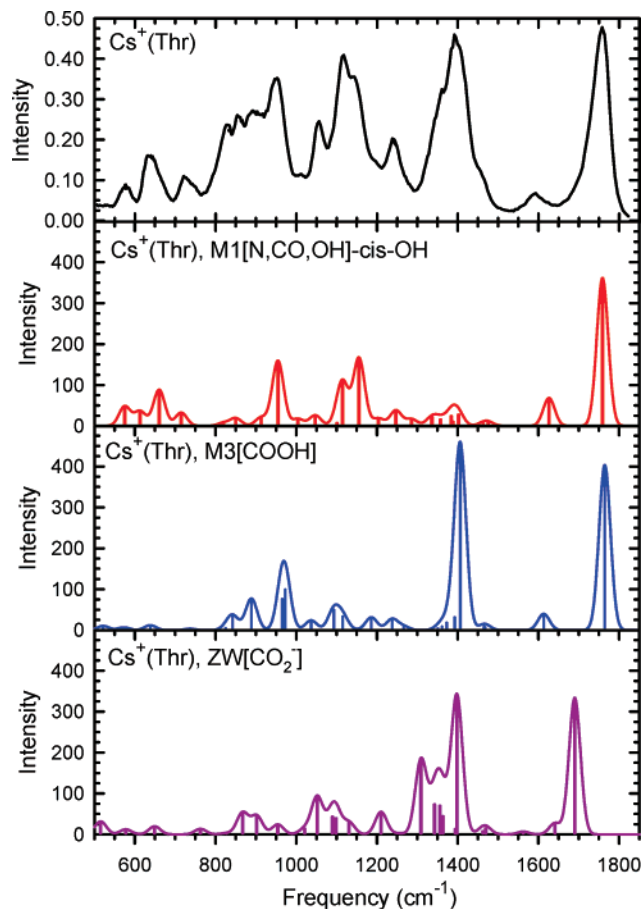


Figure 6. Comparison of the experimental IRMPD action spectrum for $Cs^+(\text{Thr})$ with IR spectra for three low-lying conformations predicted at the B3LYP/HW*/6-311+G(d,p) level of theory.

of the IRMPD spectrum in the vicinity of 1690 cm^{-1} suggests some of the ZW[CO₂⁻] conformers may also be present. The appearance of multiple conformers is consistent with the relative enthalpies and free energies calculated for this system, Table 1.

Overview. We can now provide a more global comparison of the main features in all five spectra. For the CO stretch in the M1[N,CO,OH]-*cis*-OH conformer, the predicted frequencies are 1728 , 1742 , 1749 , 1756 , and 1759 cm^{-1} for $Li^+(\text{Thr})$ – $Cs^+(\text{Thr})$, respectively, in good agreement with the blue shift observed in the spectra, Figure 1. A comparable blue shift is observed for the M3[COOH] conformer, 1725 , 1744 , 1751 , 1762 , and 1764 cm^{-1} , respectively. These shifts, which result from decreased perturbation on the CO stretch as the metal cation binding strength decreases, are clearly not conformation specific. It was noted above that the band in the $Li^+(\text{Thr})$ spectrum at 1090 cm^{-1} also shifts to the blue, reaching $\sim 1120\text{ cm}^{-1}$ for $Cs^+(\text{Thr})$. Likewise, the predicted spectral features for the M1 ground-state conformer shift from 1086 cm^{-1} for $Li^+(\text{Thr})$ to 1115 cm^{-1} for $Cs^+(\text{Thr})$. Similarly, the 1230 cm^{-1} band in $Li^+(\text{Thr})$ shifts to about 1250 cm^{-1} for $Cs^+(\text{Thr})$, in accord with the predictions of $1233\text{--}1247\text{ cm}^{-1}$, respectively. Red shifts are observed for the bands in the $Li^+(\text{Thr})$ IRMPD spectrum at 700 , 970 , and 1420 cm^{-1} . The predicted spectral features for M1[N,CO,OH]-*cis*-OH also shift to the red, to 660 , 955 , and 1402 cm^{-1} , respectively, for $Cs^+(\text{Thr})$. The band at 1160 cm^{-1} in the $Li^+(\text{Thr})$ spectrum is observed to shift to $1140\text{--}1150\text{ cm}^{-1}$ for the heavier metal cations. In the complexes of the four heavier metal cations there is only a single mode having a strong IR intensity for the M1[N,CO,OH]-*cis*-OH

conformer near this frequency, whereas for $\text{Li}^+(\text{Thr})$, there are two modes with comparable IR intensities (Figure 4), leading to the apparent blue shift in this band. Overall, the predicted trends are in remarkably good agreement with the observed spectra, suggesting that the assignment of these features to the M1 ground-state conformation is appropriate.

In contrast, the experimental spectra show that the feature at $\sim 640\text{ cm}^{-1}$ changes little with metal cation identity, whereas the predicted spectral features for the M1[N,CO,OH]-*cis*-OH conformer shift by 24 cm^{-1} : 637, 624, 618, 616, and 613 cm^{-1} for $\text{Li}^+(\text{Thr})$ - $\text{Cs}^+(\text{Thr})$, respectively. This could be because the heavier metal cation complexes include intensity from the M3-[COOH] conformer, which has a band at $640 \pm 2\text{ cm}^{-1}$ for all five metal cations. The minor band at about 1600 cm^{-1} is also observed to shift little with metal cation identity. As noted above, the position of this spectral feature is not predicted well by theory, probably because of the anharmonicity in this mode, but the mismatch is consistent for all metal cations, with predicted frequencies of 1630, 1629, 1626, 1630, and 1626 cm^{-1} for $\text{Li}^+(\text{Thr})$ - $\text{Cs}^+(\text{Thr})$, respectively.

For the M3[COOH] conformer of $\text{M}^+(\text{Thr})$, $\text{M}^+ = \text{K}^+, \text{Rb}^+$, and Cs^+ , the most diagnostic band appears at 1402, 1406, and 1407 cm^{-1} , respectively, with predicted intensities comparable to those of the band for the CO stretch at $\sim 1760\text{ cm}^{-1}$. In the experimental spectra, this band shifts little between these three metal complexes, Figure 1, and the predicted relative intensities of this band and the CO stretch are observed for the $\text{Cs}^+(\text{Thr})$ complex. The M3[COOH] conformer is also predicted to exhibit less intense bands at 893, 971, 988, and 1093 cm^{-1} for $\text{K}^+(\text{Thr})$, shifting to 891, 969, 979, and 1093 cm^{-1} for $\text{Rb}^+(\text{Thr})$ and 889, 965, 973, and 1093 cm^{-1} for $\text{Cs}^+(\text{Thr})$. The lack of a shift in these bands is consistent with experiment, but because the middle two bands are fairly close in frequency, the slight red shift in the $988\text{--}973\text{ cm}^{-1}$ band would be difficult to observe experimentally. In addition, these bands coincide with similar bands in the M1[N,CO,OH]-*cis*-OH spectrum, which shift similarly with metal cation identity. The bands observed at ~ 730 , ~ 850 , and $\sim 1050\text{ cm}^{-1}$, which do not appear in the $\text{Li}^+(\text{Thr})$ and $\text{Na}^+(\text{Thr})$ spectra, may be more diagnostic. These bands are observed to shift very little for $\text{K}^+(\text{Thr})$, $\text{Rb}^+(\text{Thr})$, and $\text{Cs}^+(\text{Thr})$. For the first two bands, this is in agreement with the predictions of bands for the M1[N,CO,OH]-*cis*-OH and M3[COOH] conformations, with M1 having a higher predicted intensity for the 730 cm^{-1} band and M3 a higher predicted intensity for the 850 cm^{-1} band, Tables S1 and S2. Likewise, shifts of only 5 and 2 cm^{-1} are predicted for bands near 1050 cm^{-1} for the M1 and ZW conformations, with the latter having a much higher predicted intensity, Table S3.

Comparisons to Results for $\text{M}^+(\text{Ser})$. A comparison of the spectra for $\text{M}^+(\text{Ser})^3$ and $\text{M}^+(\text{Thr})$, $\text{M}^+ = \text{Li}^+, \text{K}^+$, and Cs^+ , is shown in Figure 7. Experimental conditions for all spectra were essentially identical (slightly longer irradiation time for $\text{Li}^+(\text{Ser})$, 4 s compared to 3 s for all other systems), and the relative dissociation yields were similar for analogous $\text{M}^+(\text{Ser})$ and $\text{M}^+(\text{Thr})$ complexes. To a first approximation, the spectra for a particular metal ion are quite similar, and the range of conformations observed experimentally for the $\text{M}^+(\text{Ser})$ complexes matches those of the $\text{M}^+(\text{Thr})$ complexes. This result is unsurprising given the functional similarity of the two amino acids. Indeed, calculations indicate that the patterns of stability of the various conformers of the $\text{M}^+(\text{Ser})$ and $\text{M}^+(\text{Thr})$ complexes are very similar. The biggest differences occur for the high-energy M3[COOH] conformers of the lithiated and sodiated amino acids, which are relatively more stable for

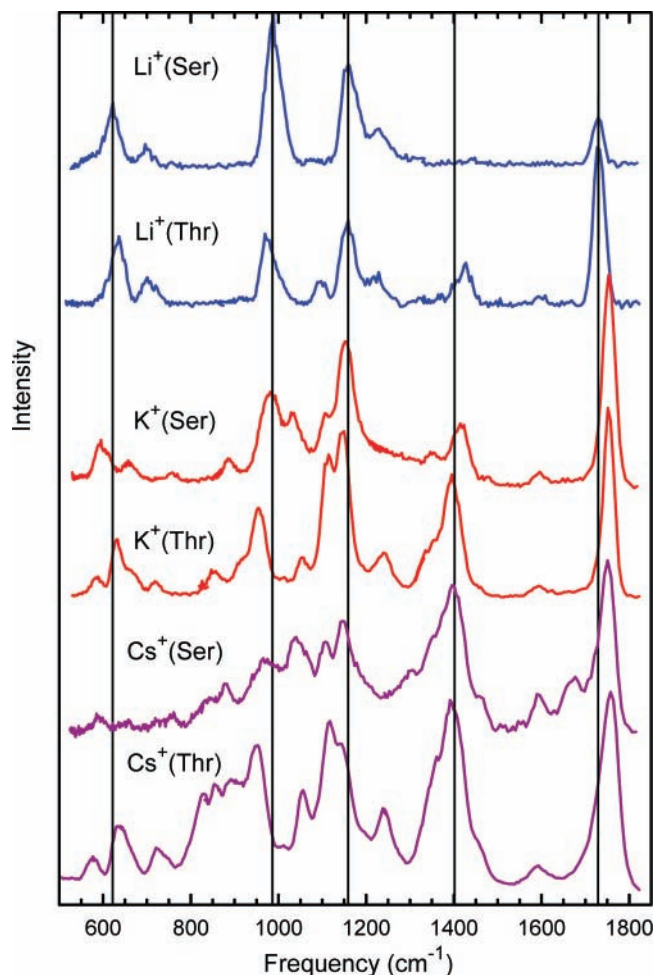


Figure 7. Comparison of the experimental IRMPD action spectra for $\text{M}^+(\text{Thr})$ and $\text{M}^+(\text{Ser})$, $\text{M}^+ = \text{Li}^+, \text{K}^+$, and Cs^+ .

$\text{M}^+(\text{Ser})$. In contrast, the M3[COOH] and ZW[CO_2^-] conformers of $\text{M}^+(\text{Thr})$ are relatively more stable for the rubidiated and cesiated amino acids but only by 1–2 kJ/mol. Despite the overall similarities, there are some differences in the spectra for the complexes of these two amino acids that are useful to examine more fully.

One notable difference is that the agreement between the predicted and experimental spectrum for $\text{Li}^+(\text{Thr})$ is more complete than observed for the $\text{Li}^+(\text{Ser})$ complex, even though the intensity maxima in these spectra are comparable, approximately 10% dissociation. Specifically, predicted bands at 1090 and 1420 cm^{-1} are observed in the spectrum for $\text{Li}^+(\text{Thr})$, whereas only hints of such bands are present in the $\text{Li}^+(\text{Ser})$ spectrum. A possible explanation for this difference is that the Thr system has a slightly lower threshold (by about 0.1–0.2 eV)³⁵ for loss of water and the aldehyde (HCHO in Ser and CH_3CHO in Thr). It is also possible that the absorption efficiency is influenced by the higher density of states in the Thr complex.

In our previous work on the IRMPD spectrum of $\text{M}^+(\text{Ser})$,³ we found that the band analogous to that observed here at 640 cm^{-1} appeared to be red shifted compared with the theoretical prediction. In both $\text{M}^+(\text{Ser})$ and $\text{M}^+(\text{Thr})$ complexes, this frequency corresponds to the wagging motion of the carboxylic acid hydrogen atom. Hence, we hypothesized that the red shift indicated that the calculations overestimate the strength of the hydrogen bond between this hydrogen atom and the carbonyl group. Similar red shifts are observed in all the $\text{M}^+(\text{Thr})$ complexes except $\text{Li}^+(\text{Thr})$, where the agreement between

experiment and theory is excellent. Some of these variations among the various systems may be associated with how the systems respond to nearby bands, whose intensities vary substantially as a function of the metal cation identity.

Other bands are observed to shift slightly between the $M^+(\text{Thr})$ and $M^+(\text{Ser})$ complexes. For example, the bands at $950\text{--}970\text{ cm}^{-1}$ in the $M^+(\text{Thr})$ spectra are shifted to the blue in $M^+(\text{Ser})$ by $10\text{--}20\text{ cm}^{-1}$. The theoretical calculations predict a systematic shift of 10 cm^{-1} , with the motion corresponding largely to the NH_2 umbrella-like motion. The observed shifts are consistent with slightly stronger bonding in the $M^+(\text{Thr})$ system. The new bands at 1050 cm^{-1} appearing in the $M^+(\text{Thr})$ spectra for the heavier metal cations, K^+ , Rb^+ , and Cs^+ are red shifted by $\sim 20\text{ cm}^{-1}$ in the $M^+(\text{Ser})$ spectra and appear to be more intense. The shifts and changes in intensity are most consistent with the $\text{ZW}[\text{CO}_2^-]$ structure, where the motion corresponds largely to a bend in the $\text{NH}\cdots\text{O}(\text{side chain})$ hydrogen bond. If the $\text{M1}[\text{N,CO,OH}]\text{-cis-OH}$ structure is considered, a similar shift can be located, but the motions change from $M^+(\text{Thr})$ to $M^+(\text{Ser})$, and the predicted intensities are the same.

For $\text{Li}^+(\text{Thr})$, the bands at 1090 and 1420 cm^{-1} have no analogues in the $\text{Li}^+(\text{Ser})$ IRMPD spectrum (although hints of absorption at these frequencies exist). The theoretical calculations for $\text{M1}[\text{N,CO,OH}]\text{-cis-OH}$ predict bands at these frequencies in both complexes but a higher IR intensity (by factors of 2 and 1.5, respectively) in $\text{Li}^+(\text{Thr})$. At 1090 cm^{-1} , the motion involved is essentially a CN stretch in both complexes, but in Thr, this mixes in the CH_3 wagging motion. Theory then predicts that this band gets more intense as the metal cation gets heavier (by a factor of about 2.5) and blue shifts. These predictions are consistent with both the $M^+(\text{Thr})$ and $M^+(\text{Ser})$ spectra. For the 1420 cm^{-1} band, the motion is an OCO bend and the intensities are predicted to get weaker as the metal cation gets heavier, in contrast to the experimental observations. This is evidence that contributions from other conformers, notably $\text{M3}[\text{COOH}]$, are probably the reason for the increase in intensity of this band in both the $M^+(\text{Thr})$ and $M^+(\text{Ser})$ IRMPD spectra.

The band at $\sim 1230\text{ cm}^{-1}$ is distinct in the $\text{Li}^+(\text{Ser})$, $\text{Li}^+(\text{Thr})$, $\text{K}^+(\text{Thr})$, and $\text{Cs}^+(\text{Thr})$ spectra and if present appears to be red shifted and less intense in the $\text{K}^+(\text{Ser})$ and $\text{Cs}^+(\text{Ser})$ spectra. The motion involved in the $\text{M1}[\text{N,CO,OH}]\text{-cis-OH}$ conformer is largely a side-chain HOC bend with contributions from HNH rock. The observations are consistent with theory, which predicts comparable intensities for the $\text{Li}^+(\text{Ser})$ and $\text{Li}^+(\text{Thr})$ complexes but higher intensity (by ~ 1.7) for $\text{Cs}^+(\text{Thr})$ compared to $\text{Cs}^+(\text{Ser})$, in part because the intensity shifts to a lower frequency band for $\text{Cs}^+(\text{Ser})$ (at 1190 cm^{-1}).

One of the key differences between the IRMPD spectra of $M^+(\text{Thr})$ and $M^+(\text{Ser})$ is the peak at 1680 cm^{-1} in $\text{Cs}^+(\text{Ser})$, although the $\text{Cs}^+(\text{Thr})$ does show weak intensity in this spectral region. As noted in our previous work,³ this peak is characteristic of the $\text{ZW}[\text{CO}_2^-]$ conformer. Theory predicts that the CO stretches of the ZW conformer in both $\text{Cs}^+(\text{Ser})$ and $\text{Cs}^+(\text{Thr})$ have nearly identical frequencies and IR intensities and that the zwitterion structure has a comparable stability compared to the $\text{M3}[\text{COOH}]$ ground state, $10\text{--}14\text{ kJ/mol}$ higher. Furthermore, the transition states between the M3 and ZW structures are calculated to have similar energies, $5\text{--}11\text{ kJ/mol}$ above M3. However, all three levels of theory find that the energies of ZW and the transition state compared to M3 are systematically higher in the $\text{Cs}^+(\text{Ser})$ system than in $\text{Cs}^+(\text{Thr})$ (by $\sim 1\text{ kJ/mol}$ for ΔH_0 and $\sim 2\text{ kJ/mol}$ for ΔG_{298}). Thus, the difference observed in the spectra could be a consequence of this or other

subtle distinctions in the potential-energy landscape separating these two conformers or perhaps between the experimental conditions for generation of the complexes.

It may seem contradictory that evidence for the ZW conformer is found even though the calculations find no energetic barrier between the ZW and M3 conformers in either the $\text{Cs}^+(\text{Ser})$ and $\text{Cs}^+(\text{Thr})$ complexes once zero-point energies are included. In thinking about this observation, it can be realized that there must still be a phase space limit (lower density of states) between the conformers because of the barrier along the electronic surface. This plausibly allows the system to exist in the ZW conformation for long enough times to allow IRMPD. A different way of thinking of this same dynamic issue is to appreciate that the hydrogen stretching motion that converts between the ZW and M3 conformers is high frequency, calculated to be 3133 cm^{-1} (ZPE = 18.7 kJ/mol) for M3 of $\text{Cs}^+(\text{Thr})$ and 2818 cm^{-1} (ZPE = 16.9 kJ/mol) for ZW of $\text{Cs}^+(\text{Thr})$. Thus, the former ZPE lies above or close to the height of the barrier, 18.7 , 13.9 , and 19.3 kJ/mol above the M3 conformer without ZPE correction at the B3LYP, B3P86, and MP2(full) levels of theory, respectively. Viewed from the ZW potential well, the barrier heights without ZPE correction are 8.0 , 3.9 , and 7.0 kJ/mol , well below the 16.9 kJ/mol ZPE of the reaction coordinate for M3–ZW interconversion. Clearly, the potential surface along this coordinate is no longer harmonic, such that the calculated frequencies are unlikely to be accurate; however, it seems plausible that the ground-state wavefunction for this vibration includes components in both the M3 and ZW potential-energy wells, thereby allowing IR absorption in the orthogonal degrees of freedom probed in these experiments for both conformers.

Conclusions

IRMPD action spectra of the alkali-metal cationized amino acid threonine in the region of $550\text{--}1800\text{ cm}^{-1}$ have been obtained for five alkali-metal cations, $M^+ = \text{Li}^+$, Na^+ , K^+ , Rb^+ , and Cs^+ . Comparison with IR spectra calculated at the B3LYP/6-311+G(d,p) ($M^+ = \text{Li}^+$, Na^+ , and K^+) and B3LYP/HW*/6-311+G(d,p) ($M^+ = \text{Rb}^+$ and Cs^+) levels of theory allow the conformations present in the experiment to be identified. The experimental results suggest that only the tridentate $\text{M1}[\text{N,CO,OH}]\text{-cis-OH}$ conformation is present for the $\text{Li}^+(\text{Thr})$ and $\text{Na}^+(\text{Thr})$ complexes, in agreement with the predicted ground states of these complexes. For the $\text{K}^+(\text{Thr})$, $\text{Rb}^+(\text{Thr})$, and $\text{Cs}^+(\text{Thr})$ complexes, the presence of the $\text{M3}[\text{COOH}]$ conformer along with the $\text{M1}[\text{N,CO,OH}]\text{-cis-OH}$ conformer is indicated, and there are hints that the zwitterionic conformer, $\text{ZW}[\text{CO}_2^-]$, may also be present. Theory finds that the $\text{M3}[\text{COOH}]$ conformer becomes the ground state for the heavier metal systems, consistent with its observation in their spectra. The large change in the relative stabilities of the $\text{M1}[\text{N,CO,OH}]\text{-cis-OH}$ and $\text{M3}[\text{COOH}]$ conformers can be rationalized on the basis of the strength of the M^+ –amine interaction as a function of the metal cation.^{11,21} The smaller metal cations bind relatively more strongly to the amine, favoring the M1 structure, whereas the heavier more diffuse metal cations prefer binding to the carboxylic acid site. These results parallel those observed for the analogous $M^+(\text{Ser})$ complexes.³ Other more subtle differences in the IRMPD spectra for $M^+(\text{Ser})$ and $M^+(\text{Thr})$ are also well described by theory in most cases.

Acknowledgment. This work is part of the research program of FOM, which is financially supported by the Nederlandse Organisatie voor Wetenschappelijk Onderzoek (NWO). Ad-

ditional financial support was provided by the National Science Foundation, Grants PIRE-0730072, CHE-0451477 and CHE-0748790 (P.B.A.), and CHE-0528262 (M.T.R.). The skillful assistance of the FELIX staff is gratefully acknowledged.

Supporting Information Available: Five figures showing the breakdown of the experimental spectra for $\text{Li}^+(\text{Thr})$ and $\text{Na}^+(\text{Thr})$ into individual product ions (Figure S1) and a comparison between the experimental IRMPD spectrum and theoretically predicted IR spectra of seven low-lying conformations of $\text{Na}^+(\text{Thr})$, $\text{K}^+(\text{Thr})$, and $\text{Rb}^+(\text{Thr})$, and $\text{Cs}^+(\text{Thr})$ (Figures S2–S5); three tables (S1–S3) provide the vibrational frequencies and IR intensities for the M1[N,CO,OH]-*cis*-OH, M3-[COOH], and ZW[CO₂⁻] conformations for $\text{M}^+(\text{Thr})$ calculated at the B3LYP/6-311+G(d,p) ($\text{M}^+ = \text{Li}^+, \text{Na}^+, \text{and K}^+$) or B3LYP/HW*/6-311+G(d,p) ($\text{M}^+ = \text{Rb}^+ \text{ and } \text{Cs}^+$) levels of theory; one table (S4) provides vibrational frequencies and IR intensities for the M1[N,CO,OH]-*trans*-OH, M8[CO,OH], M1-[N,CO], and M5[N,OH,OH] conformations for $\text{Li}^+(\text{Thr})$ calculated at the B3LYP/6-311+G(d,p) level of theory. This material is available free of charge via the Internet at <http://pubs.acs.org>.

References and Notes

- Dashper, S. G.; Brownfield, L.; Slakeski, N.; Zilm, P. S.; Rogers, A. H.; Reynolds, E. C. *J. Bacteriol.* **2001**, *183*, 4142–4148.
- Ye, S. J.; Clark, A. A.; Armentrout, P. B. *J. Phys. Chem. B*, submitted for publication.
- Armentrout, P. B.; Rodgers, M. T.; Oomens, J.; Steill, J. D. *J. Phys. Chem. A* **2008**, *112*, 2248–2257.
- Polfer, N. C.; Oomens, J.; Dunbar, R. C. *Phys. Chem. Chem. Phys.* **2006**, *8*, 2744–2751.
- Bush, M. F.; Forbes, M. W.; Jockusch, R. A.; Oomens, J.; Polfer, N. C.; Saykally, R. J.; Williams, E. R. *J. Phys. Chem. A* **2007**, *111*, 7753–7760.
- Forbes, M. W.; Bush, M. F.; Polfer, N. C.; Oomens, J.; Dunbar, R. C.; Williams, E. R.; Jockusch, R. A. *J. Phys. Chem. A* **2007**, *111*, 11759–11770.
- Valle, J. J.; Eyler, J. R.; Oomens, J.; Moore, D. T.; van der Meer, A. F. G.; von Helden, G.; Meijer, G.; Hendrickson, C. L.; Marshall, A. G.; Blakney, G. T. *Rev. Sci. Instrum.* **2005**, *76*, 023103.
- Polfer, N. C.; Oomens, J.; Moore, D. T.; von Helden, G.; Meijer, G.; Dunbar, R. C. *J. Am. Chem. Soc.* **2006**, *128*, 517–525.
- Polfer, N. C.; Oomens, J. *Phys. Chem. Chem. Phys.* **2007**, *9*, 3804–3817.
- Oepts, D.; van der Meer, A. F. G.; van Amersfoort, P. W. *Infrared Phys. Technol.* **1995**, *36*, 297–308.
- Moision, R. M.; Armentrout, P. B. *J. Phys. Chem. A* **2002**, *106*, 10350–10362.
- Pearlman, D. A.; Case, D. A.; Caldwell, J. W.; Ross, W. R.; Cheatham, T. E.; DeBolt, S.; Ferguson, D.; Seibel, G.; Kollman, P. *Comp. Phys. Commun.* **1995**, *91*, 1–41.
- Bylaska, E. J.; de Jong, W. A.; Kowalski, K.; Straatsma, T. P.; Valiev, M.; Wang, D.; Aprà, E.; Windus, T. L.; Hirata, S.; Hackler, M. T.; Zhao, Y.; Fan, P.-D.; Harrison, R. J.; Dupuis, M.; Smith, D. M. A.; Nieplocha, J.; Tipparaju, V.; Krishnan, M.; Auer, A. A.; Nooijen, M.; Brown, E.; Cisneros, G.; Fann, G. I.; Früchtl, H.; Garza, J.; Hirao, K.; Kendall, R.; Nichols, J. A.; Tsemekhman, K.; Wolinski, K.; Anchell, J.; Bernholdt, D.; Borowski, P.; Clark, T.; Clerc, D.; Dachselt, H.; Deegan, M.; Dyall, K.; Elwood, D.; Glendening, E.; Gutowski, M.; Hess, A.; Jaffe, J.; Johnson, B.; Ju, J.; Kobayashi, R.; Kutteh, R.; Lin, Z.; Littlefield, R.; Long, X.; Meng, B.; Nakajima, T.; Niu, S.; Pollack, L.; Rosing, M.; Sandrone, G.; Stave, M.; Taylor, H.; Thomas, G.; Lenthe, J. v.; Wong, A.; Zhang, Z., *NWChem, A Computational Chemistry Package for Parallel Computers*, Version 4.5; Pacific Northwest National Laboratory: Richland, WA, 2003.
- Roothaan, C. C. *Rev. Mod. Phys.* **1951**, *23*, 69–89.
- Binkley, J. S.; Pople, J. A.; Hehre, W. J. *J. Am. Chem. Soc.* **1980**, *102*, 939–947.
- Frisch, M. J.; Trucks, G. W.; Schlegel, H. B.; Scuseria, G. E.; Robb, M. A.; Cheeseman, J. R.; Montgomery, J., J. A.; Vreven, T.; Kudin, K. N.; Burant, J. C.; Millam, J. M.; Iyengar, S. S.; Tomasi, J.; Barone, V.; Mennucci, B.; Cossi, M.; Scalmani, G.; Rega, N.; Petersson, G. A.; Nakatsuji, H.; Hada, M.; Ehara, M.; Toyota, K.; Fukuda, R.; Hasegawa, J.; Ishida, M.; Nakajima, T.; Honda, Y.; Kitao, O.; Nakai, H.; Klene, M.; Li, X.; Knox, J. E.; Hratchian, H. P.; Cross, J. B.; Bakken, V.; Adamo, C.; Jaramillo, J.; Gomperts, R.; Stratmann, R. E.; Yazyev, O.; Austin, A. J.; Cammi, R.; Pomelli, C.; Ochterski, J. W.; Ayala, P. Y.; Morokuma, K.; Voth, G. A.; Salvador, P.; Dannenberg, J. J.; Zakrzewski, V. G.; Dapprich, S.; Daniels, A. D.; Strain, M. C.; Farkas, O.; Malick, D. K.; Rabuck, A. D.; Raghavachari, K.; Foresman, J. B.; Ortiz, J. V.; Cui, Q.; Baboul, A. G.; Clifford, S.; Cioslowski, J.; Stefanov, B. B.; Liu, G.; Liashenko, A.; Piskorz, P.; Komaromi, I.; Martin, R. L.; Fox, D. J.; Keith, T.; Al-Laham, M. A.; Peng, C. Y.; Nanayakkara, A.; Challacombe, M.; Gill, P. M. W.; Johnson, B.; Chen, W.; Wong, M. W.; Gonzalez, C.; Pople, J. A., *Gaussian 03*, Revision D.01; Gaussian, Inc.: Pittsburgh, PA, 2005.
- Becke, A. D. *J. Chem. Phys.* **1993**, *98*, 5648–5652.
- Ditchfield, R.; Hehre, W. J.; Pople, J. A. *J. Chem. Phys.* **1971**, *54*, 724–728.
- McLean, A. D.; Chandler, G. S. *J. Chem. Phys.* **1980**, *72*, 5639–5648.
- Krishnan, R.; Binkley, J. S.; Seeger, R.; Pople, J. A. *J. Chem. Phys.* **1980**, *72*, 650–654.
- Moision, R. M.; Armentrout, P. B. *Phys. Chem. Chem. Phys.* **2004**, *6*, 2588–2599.
- Foresman, J. B.; Frisch, A. E. *Exploring Chemistry with Electronic Structure Methods*, 2nd ed.; Gaussian, Inc.: Pittsburgh, PA, 1996.
- Hay, P. J.; Wadt, W. R. *J. Chem. Phys.* **1985**, *82*, 299–310.
- Glendening, E. D.; Feller, D.; Thompson, M. A. *J. Am. Chem. Soc.* **1994**, *116*, 10657–10669.
- Oomens, J.; Moore, D. T.; Meijer, G.; von Helden, G. *Phys. Chem. Chem. Phys.* **2004**, *6*, 710–718.
- Oomens, J.; Sartakov, B. G.; Meijer, G.; von Helden, G. *Int. J. Mass Spectrom.* **2006**, *254*, 1–19.
- Rodríguez-Santiago, L.; Sodupe, M.; Tortajada, J. *J. Phys. Chem. A* **2001**, *105*, 5340–5347.
- Pulkkinen, S.; Noguera, M.; Rodríguez-Santiago, L.; Sodupe, M.; Bertran, J. *Chem. Eur. J.* **2000**, *6*, 4393–4399.
- Jensen, F. *J. Am. Chem. Soc.* **1992**, *114*, 9533–9537.
- Wilson, R. G.; Brewer, G. R. *Ion Beams with Applications to Ion Implantation*; Wiley: New York, 1973.
- Peng, C. Y.; Schlegel, H. B. *Israel J. Chem.* **1994**, *33*, 449.
- Moision, R. M.; Armentrout, P. B. Manuscript in preparation.
- Kapota, C.; Lemaire, J.; Maitre, P.; Ohanessian, G. *J. Am. Chem. Soc.* **2004**, *126*, 1836–1842.
- Sinclair, W. E.; Pratt, D. W. *J. Chem. Phys.* **1996**, *105*, 7942–7956.
- Ye, S. J.; Armentrout, P. B. *J. Phys. Chem. B*, submitted for publication.